Calculating Accurate Waveforms for LIGO and LISA Data Analysis

Lee Lindblom

Theoretical Astrophysics, Caltech

HEPL-KIPAC Seminar, Stanford – 17 November 2009

Results from the Caltech/Cornell Numerical Relativity Collaboration.

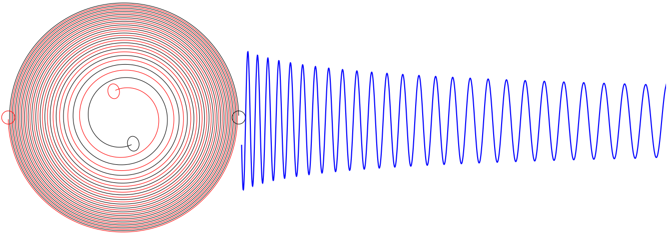

Motivation: Gravitational Wave Astronomy

- Recent work in numerical relativity is aimed at providing model waveforms for gravitational wave (GW) astronomy (LIGO, etc.).
- Binary black hole systems emit large amounts of GW as the holes inspiral and ultimately merge. These are expected to be among the strongest sources detectable by LIGO.

Motivation: Gravitational Wave Astronomy

- Recent work in numerical relativity is aimed at providing model waveforms for gravitational wave (GW) astronomy (LIGO, etc.).
- Binary black hole systems emit large amounts of GW as the holes inspiral and ultimately merge. These are expected to be among the strongest sources detectable by LIGO.
- Numerical waveforms may be useful in detection (to construct better data filters), and/or in modeling detected signals.

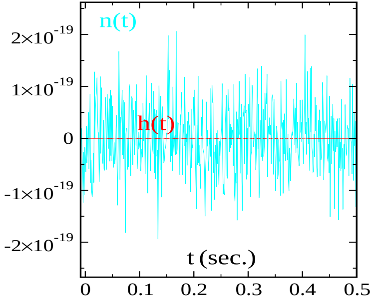

Motivation: Gravitational Wave Astronomy

- Recent work in numerical relativity is aimed at providing model waveforms for gravitational wave (GW) astronomy (LIGO, etc.).
- Binary black hole systems emit large amounts of GW as the holes inspiral and ultimately merge. These are expected to be among the strongest sources detectable by LIGO.
- Numerical waveforms may be useful in detection (to construct better data filters), and/or in modeling detected signals.

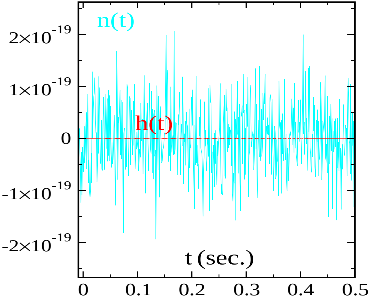

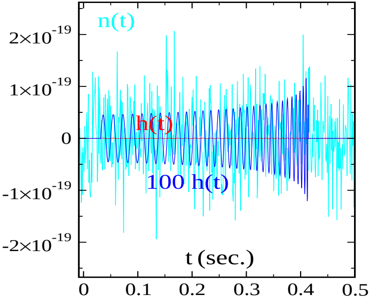

Gravitational Wave Data Analysis

- Signals $h_s(t)$ are detected in the noisy LIGO data by projecting them onto a model waveforms $h_m(\lambda, t)$.
- The measured signal-to-noise ratio, $\rho_m(\lambda)$, is maximized by adjusting the model waveform parameters λ.

$$\rho_m(\lambda) = 4\int_0^\infty \frac{Re[h_s(f)h_m^*(f,\lambda)]}{S_n(f)}df \left[4\int_0^\infty \frac{|h_m(f,\lambda)|^2}{S_n(f)}df\right]^{-1/2}$$

Gravitational Wave Data Analysis

- Signals $h_s(t)$ are detected in the noisy LIGO data by projecting them onto a model waveforms $h_m(\lambda, t)$.
- The measured signal-to-noise ratio, $\rho_m(\lambda)$, is maximized by adjusting the model waveform parameters λ.

$$\rho_m(\lambda) = 4\int_0^\infty \frac{Re[h_s(f)h_m^*(f,\lambda)]}{S_n(f)}df \left[4\int_0^\infty \frac{|h_m(f,\lambda)|^2}{S_n(f)}df\right]^{-1/2}$$

- A detection occurs whenever a signal is present that matches a model waveform with $\rho_m(\lambda) > \rho_{\min}$. For LIGO searches $\rho_{\min} \approx 8$.

Gravitational Wave Data Analysis

- Signals $h_s(t)$ are detected in the noisy LIGO data by projecting them onto a model waveforms $h_m(\lambda, t)$.
- The measured signal-to-noise ratio, $\rho_m(\lambda)$, is maximized by adjusting the model waveform parameters λ.

$$\rho_m(\lambda) = 4\int_0^\infty \frac{Re[h_s(f)h_m^*(f,\lambda)]}{S_n(f)}df\left[4\int_0^\infty \frac{|h_m(f,\lambda)|^2}{S_n(f)}df\right]^{-1/2}$$

- A detection occurs whenever a signal is present that matches a model waveform with $\rho_m(\lambda) > \rho_{\min}$. For LIGO searches $\rho_{\min} \approx 8$.

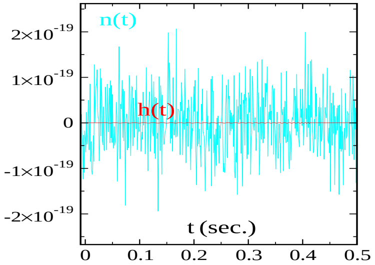

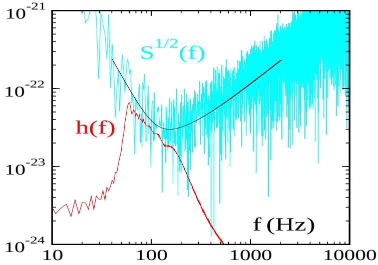

How Accurate Must Model Waveforms Be?

- Write the model waveform as $h_m(f) = h_s(f)e^{\delta\chi_m(f)+i\delta\Phi_m(f)}$, where $\delta\chi_m(f)$ and $\delta\Phi_m(f)$ represent errors in its amplitude and phase.

How Accurate Must Model Waveforms Be?

- Write the model waveform as $h_m(f) = h_s(f)e^{\delta\chi_m(f)+i\delta\Phi_m(f)}$, where $\delta\chi_m(f)$ and $\delta\Phi_m(f)$ represent errors in its amplitude and phase.
- Inaccurate model waveforms degrade the measured signal-to-noise ratios $\rho_m(\lambda)$, resulting in missed detections.
- To ensure that the loss rate of detections does not exceed 10%, the waveform errors must not exceed:

$$0.01 \gtrsim \left(\overline{\delta\chi_m}\right)^2 + \left(\overline{\delta\Phi_m}\right)^2 \equiv \int_0^\infty \left[(\delta\chi_m)^2 + (\delta\Phi_m)^2\right] \frac{4|h_s|^2}{\rho^2 S_n} df.$$

How Accurate Must Model Waveforms Be?

- Write the model waveform as $h_m(f) = h_s(f)e^{\delta\chi_m(f)+i\delta\Phi_m(f)}$, where $\delta\chi_m(f)$ and $\delta\Phi_m(f)$ represent errors in its amplitude and phase.
- Inaccurate model waveforms degrade the measured signal-to-noise ratios $\rho_m(\lambda)$, resulting in missed detections.
- To ensure that the loss rate of detections does not exceed 10%, the waveform errors must not exceed:

$$0.01 \gtrsim \left(\overline{\delta\chi_m}\right)^2 + \left(\overline{\delta\Phi_m}\right)^2 \equiv \int_0^\infty \left[(\delta\chi_m)^2 + (\delta\Phi_m)^2\right] \frac{4|h_s|^2}{\rho^2 S_n} df.$$

- Physical properties of the GW source are measured by adjusting the model waveform parameters $h_m(f,\lambda)$ to achieve the largest measured signal-to-noise $\rho_m(\lambda)$.

How Accurate Must Model Waveforms Be?

- Write the model waveform as $h_m(f) = h_s(f)e^{\delta\chi_m(f)+i\delta\Phi_m(f)}$, where $\delta\chi_m(f)$ and $\delta\Phi_m(f)$ represent errors in its amplitude and phase.
- Inaccurate model waveforms degrade the measured signal-to-noise ratios $\rho_m(\lambda)$, resulting in missed detections.
- To ensure that the loss rate of detections does not exceed 10%, the waveform errors must not exceed:

$$0.01 \gtrsim \left(\overline{\delta\chi_m}\right)^2 + \left(\overline{\delta\Phi_m}\right)^2 \equiv \int_0^\infty \left[(\delta\chi_m)^2 + (\delta\Phi_m)^2\right] \frac{4|h_s|^2}{\rho^2 S_n} df.$$

- Physical properties of the GW source are measured by adjusting the model waveform parameters $h_m(f,\lambda)$ to achieve the largest measured signal-to-noise $\rho_m(\lambda)$.
- To ensure the errors in the measured parameters λ are dominated by the intrinsic detector noise $S_n(f)$ rather than model waveform error, the waveform errors must not exceed:

$$\frac{1}{4\rho^2_{\max}} \approx 2.5 \times 10^{-5} \gtrsim \left(\overline{\delta\chi_m}\right)^2 + \left(\overline{\delta\Phi_m}\right)^2.$$

How Are Accurate Waveforms Calculated?

Computational Challanges:

- Dynamics of binary black hole problem is driven by delicate adjustments to orbit due to emission of gravitational waves.
- Very big computational problem:
  - Must evolve ~ 50 dynamical fields (spacetime metric plus all first derivatives).
  - Must accurately resolve features on many scales from black hole horizons $r \sim GM/c^2$ to emitted waves $r \sim 100GM/c^2$.
  - Many grid points are required $\gtrsim 10^6$ even if points are located optimally.

How Are Accurate Waveforms Calculated?

Computational Challanges:

- Dynamics of binary black hole problem is driven by delicate adjustments to orbit due to emission of gravitational waves.
- Very big computational problem:
  - Must evolve ~ 50 dynamical fields (spacetime metric plus all first derivatives).
  - Must accurately resolve features on many scales from black hole horizons $r \sim GM/c^2$ to emitted waves $r \sim 100GM/c^2$.
  - Many grid points are required $\gtrsim 10^6$ even if points are located optimally.
- Most representations of the Einstein equations have mathematically ill-posed initial value problems.
- Constraint violating instabilities destroy stable numerical solutions in many well-posed forms of the equations.

Outline of Remainder of Talk:

- Interesting Features of the Caltech/Cornell code:
  - Constraint Damping.
  - Pseudo-Spectral Methods.
  - Horizon Tracking and Conforming Grid Structures..
  - Damped Harmonic Gauge Conditions.
- Results:
  - Generic Mergers.
  - Accurate BBH waveforms.

Gauge and Constraints in Electromagnetism

- The usual representation of the vacuum Maxwell equations split into evolution equations and constraints:

$$\begin{aligned} \partial_t \vec{E} &= \vec{\nabla} \times \vec{B}, & \qquad \nabla \cdot \vec{E} &= 0, \\ \partial_t \vec{B} &= -\vec{\nabla} \times \vec{E}, & \qquad \nabla \cdot \vec{B} &= 0. \end{aligned}$$

  These equations are often written in the more compact 4-dimensional notation: $\nabla^a F_{ab} = 0$ and $\nabla_{[a} F_{bc]} = 0$, where F_{ab} has components $\vec{E}$ and $\vec{B}$.

Gauge and Constraints in Electromagnetism

- The usual representation of the vacuum Maxwell equations split into evolution equations and constraints:

$$\partial_t \vec{E} = \vec{\nabla} \times \vec{B}, \qquad \nabla \cdot \vec{E} = 0,$$
$$\partial_t \vec{B} = -\vec{\nabla} \times \vec{E}, \qquad \nabla \cdot \vec{B} = 0.$$

  These equations are often written in the more compact 4-dimensional notation: $\nabla^a F_{ab} = 0$ and $\nabla_{[a} F_{bc]} = 0$, where F_{ab} has components $\vec{E}$ and $\vec{B}$.
- Maxwell's equations are often re-expressed in terms of a vector potential $F_{ab} = \nabla_a A_b - \nabla_b A_a$:

$$\nabla^a \nabla_a A_b - \nabla_b \nabla^a A_a = 0.$$

Gauge and Constraints in Electromagnetism

- The usual representation of the vacuum Maxwell equations split into evolution equations and constraints:

$$\partial_t \vec{E} = \vec{\nabla} \times \vec{B}, \qquad \nabla \cdot \vec{E} = 0,$$
$$\partial_t \vec{B} = -\vec{\nabla} \times \vec{E}, \qquad \nabla \cdot \vec{B} = 0.$$

  These equations are often written in the more compact 4-dimensional notation: $\nabla^a F_{ab} = 0$ and $\nabla_{[a} F_{bc]} = 0$, where F_{ab} has components $\vec{E}$ and $\vec{B}$.
- Maxwell's equations are often re-expressed in terms of a vector potential $F_{ab} = \nabla_a A_b - \nabla_b A_a$:

$$\nabla^a \nabla_a A_b - \nabla_b \nabla^a A_a = 0.$$

- This form of Maxwell's equations is manifestly hyperbolic as long as the gauge is chosen correctly, e.g., let $\nabla^a A_a = H(x, t)$, giving:

$$\nabla^a \nabla_a A_b \equiv \left(-\partial_t^2 + \partial_x^2 + \partial_y^2 + \partial_z^2\right) A_b = \nabla_b H.$$

Constraint Damping

- Where are the constraints: $\nabla^a \nabla_a A_b = \nabla_b H$?

Constraint Damping

- Where are the constraints: $\nabla^a\nabla_a A_b = \nabla_b H$?
- Gauge condition becomes a constraint: $0 = \mathcal{C} \equiv \nabla^a A_a - H$.
- Maxwell's equations imply that this constraint is preserved:

$$\nabla^a\nabla_a \mathcal{C} = 0.$$

Constraint Damping

- Where are the constraints: $\nabla^a \nabla_a A_b = \nabla_b H$?
- Gauge condition becomes a constraint: $0 = \mathcal{C} \equiv \nabla^a A_a - H$.
- Maxwell's equations imply that this constraint is preserved:

$$\nabla^a \nabla_a \mathcal{C} = 0.$$

- Modify evolution equations by adding multiples of the constraints:

$$\nabla^a \nabla_a A_b = \nabla_b H + \gamma_0 t_b \mathcal{C} = \nabla_b H + \gamma_0 t_b (\nabla^a A_a - H).$$

- These changes also affect the constraint evolution equation,

$$\nabla^a \nabla_a \mathcal{C} - \gamma_0 t^b \nabla_b \mathcal{C} = 0,$$

so constraint violations are damped when $\gamma_0 > 0$.

Constraint Damped Einstein System

- "Generalized Harmonic" form of Einstein's equations have properties similar to Maxwell's equations:
  - Gauge (coordinate) conditions are imposed by specifying the divergence of the spacetime metric: $\partial_a g^{ab} = H^b + \ldots$
  - Evolution equations become manifestly hyperbolic: $\Box g_{ab} = \ldots$
  - Gauge conditions become constraints.
  - Constraint damping terms can be added which make numerical evolutions stable.

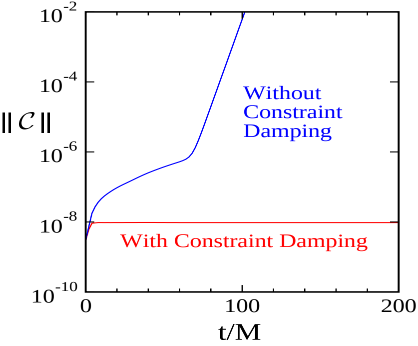

Numerical Solution of Evolution Equations

$$\partial_t u = F(u, \partial_x u, x, t).$$

- Choose a grid of spatial points, x_n.

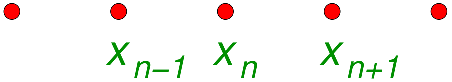

Numerical Solution of Evolution Equations

$$\partial_t u = F(u, \partial_x u, x, t).$$

- Choose a grid of spatial points, x_n.
- Evaluate the function u on this grid: $u_n(t) = u(x_n, t)$.

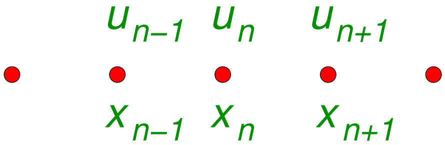

Numerical Solution of Evolution Equations

$$\partial_t u = F(u, \partial_x u, x, t).$$

- Choose a grid of spatial points, x_n.
- Evaluate the function u on this grid: $u_n(t) = u(x_n, t)$.

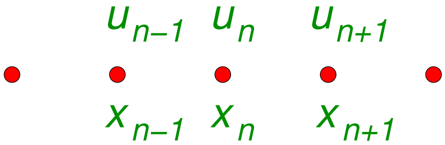

- Approximate the spatial derivatives at the grid points $\partial_x u(x_n) = \sum_k D_{nk} u_k$.

Numerical Solution of Evolution Equations

$$\partial_t u = F(u, \partial_x u, x, t).$$

- Choose a grid of spatial points, x_n.
- Evaluate the function u on this grid: $u_n(t) = u(x_n, t)$.

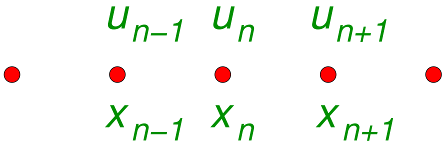

- Approximate the spatial derivatives at the grid points

$$\partial_x u(x_n) = \sum_k D_{nk} u_k.$$

- Evaluate F at the grid points x_n in terms of the u_k: $F(u_k, x_n, t)$.

Numerical Solution of Evolution Equations

$$\partial_t u = F(u, \partial_x u, x, t).$$

- Choose a grid of spatial points, x_n.
- Evaluate the function u on this grid: $u_n(t) = u(x_n, t)$.

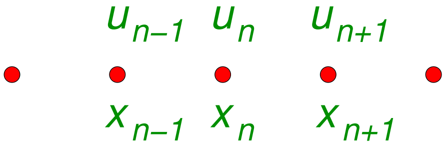

- Approximate the spatial derivatives at the grid points
  $\partial_x u(x_n) = \sum_k D_{n\,k} u_k$.
- Evaluate F at the grid points x_n in terms of the u_k: $F(u_k, x_n, t)$.
- Solve the coupled system of ordinary differential equations,

$$\frac{du_n(t)}{dt} = F[u_k(t), x_n, t],$$

  using standard numerical methods (e.g. Runge-Kutta).

Basic Numerical Methods

- Different numerical methods use different ways of choosing the grid points x_n, and different expressions for the spatial derivatives

$$\partial_x u(u_n) = \sum_k D_{n\,k} u_k.$$

Basic Numerical Methods

- Different numerical methods use different ways of choosing the grid points x_n, and different expressions for the spatial derivatives

$$\partial_x u(u_n) = \sum_k D_{n\,k} u_k.$$

- Most numerical groups use finite difference methods:
  - Uniformly spaced grids: $x_n - x_{n-1} = \Delta x =$ constant.
  - Use Taylor expansions to obtain the needed expressions for $\partial_x u$:

$$\partial_x u(x_n) = \frac{u_{n+1} - u_{n-1}}{2\Delta x} + \mathcal{O}(\Delta x^2).$$

Basic Numerical Methods

- Different numerical methods use different ways of choosing the grid points x_n, and different expressions for the spatial derivatives

$$\partial_x u(u_n) = \sum_k D_{n\,k} u_k.$$

- Most numerical groups use finite difference methods:
  - Uniformly spaced grids: $x_n - x_{n-1} = \Delta x =$ constant.
  - Use Taylor expansions to obtain the needed expressions for $\partial_x u$:

$$\partial_x u(x_n) = \frac{u_{n+1} - u_{n-1}}{2\Delta x} + \mathcal{O}(\Delta x^2).$$

- Grid spacing decreases as the number of grid points N increases, $\Delta x \sim 1/N$. Errors in finite difference methods scale as N^{-p}.

Basic Numerical Methods II

- A few groups (including ours) use pseudo-spectral methods.

Basic Numerical Methods II

- A few groups (including ours) use pseudo-spectral methods.
- Represent functions as finite sums: $u(x,t) = \sum_{k=0}^{N-1} \tilde{u}_k(t) e^{ikx}$.
- Choose grid points x_n to allow exact (and efficient) inversion of the series: $\tilde{u}_k(t) = \sum_{n=0}^{N-1} w_n \, u(x_n, t) e^{-ikx_n}$.

Basic Numerical Methods II

- A few groups (including ours) use pseudo-spectral methods.
- Represent functions as finite sums: $u(x,t) = \sum_{k=0}^{N-1} \tilde{u}_k(t) e^{ikx}$.
- Choose grid points x_n to allow exact (and efficient) inversion of the series: $\tilde{u}_k(t) = \sum_{n=0}^{N-1} w_n\, u(x_n,t) e^{-ikx_n}$.
- Obtain derivative formulas by differentiating the series: $\partial_x u(x_n,t) = \sum_{k=0}^{N-1} \tilde{u}_k(t) \partial_x e^{ikx_n} = \sum_{m=0}^{N-1} D_{n\,m}\, u(x_m,t)$.

Basic Numerical Methods II

- A few groups (including ours) use pseudo-spectral methods.
- Represent functions as finite sums: $u(x,t) = \sum_{k=0}^{N-1} \tilde{u}_k(t) e^{ikx}$.
- Choose grid points x_n to allow exact (and efficient) inversion of the series: $\tilde{u}_k(t) = \sum_{n=0}^{N-1} w_n\, u(x_n,t) e^{-ikx_n}$.
- Obtain derivative formulas by differentiating the series: $\partial_x u(x_n,t) = \sum_{k=0}^{N-1} \tilde{u}_k(t) \partial_x e^{ikx_n} = \sum_{m=0}^{N-1} D_{n\,m}\, u(x_m,t)$.
- Errors in spectral methods are dominated by the size of $\tilde{u}_N$.
- Estimate the errors (for Fourier series of *smooth* functions):

$$\begin{aligned}\tilde{u}_N &= \frac{1}{2\pi}\int_{-\pi}^{\pi} u(x) e^{-iNx} dx \\ &\leq \frac{1}{N^p} \max \left| \frac{d^p u(x)}{dx^p} \right| .\end{aligned}$$

Basic Numerical Methods II

- A few groups (including ours) use pseudo-spectral methods.
- Represent functions as finite sums: $u(x,t) = \sum_{k=0}^{N-1} \tilde{u}_k(t) e^{ikx}$.
- Choose grid points x_n to allow exact (and efficient) inversion of the series: $\tilde{u}_k(t) = \sum_{n=0}^{N-1} w_n \, u(x_n,t) e^{-ikx_n}$.
- Obtain derivative formulas by differentiating the series: $\partial_x u(x_n,t) = \sum_{k=0}^{N-1} \tilde{u}_k(t) \partial_x e^{ikx_n} = \sum_{m=0}^{N-1} D_{n\,m} \, u(x_m,t)$.
- Errors in spectral methods are dominated by the size of $\tilde{u}_N$.
- Estimate the errors (for Fourier series of *smooth* functions):

$$\begin{aligned} \tilde{u}_N &= \frac{1}{2\pi} \int_{-\pi}^{\pi} u(x) e^{-iNx} dx \\ &\leq \frac{1}{N^p} \max \left| \frac{d^p u(x)}{dx^p} \right|. \end{aligned}$$

- Errors in spectral methods decrease faster than any power of N.

Comparing Different Numerical Methods

- Wave propagation with second-order finite difference method:

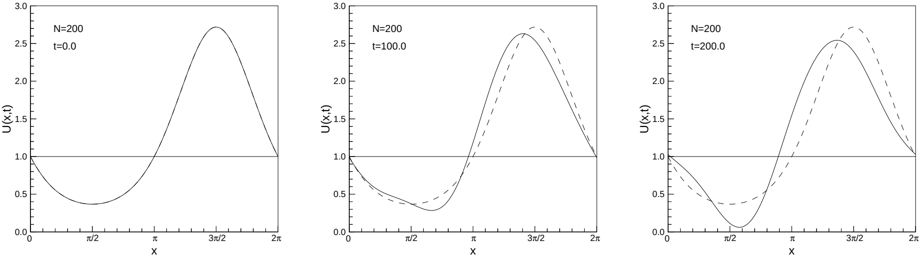

Figures from Hesthaven, Gottlieb, & Gottlieb (2007).

Comparing Different Numerical Methods

- Wave propagation with second-order finite difference method:

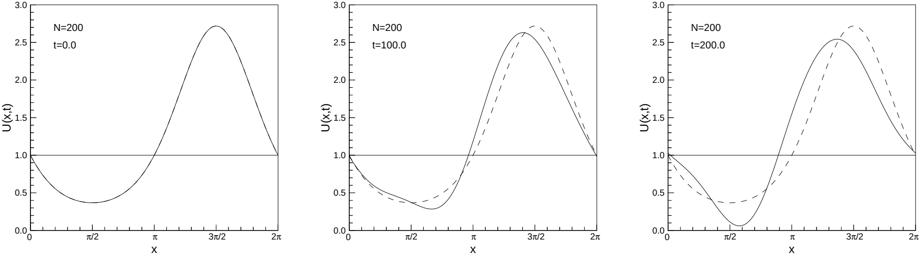

- Wave propagation with spectral method:

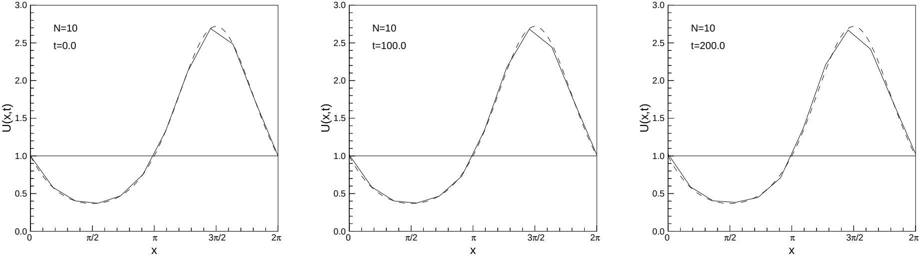

Figures from Hesthaven, Gottlieb, & Gottlieb (2007).

Caltech/Cornell Spectral Einstein Code (SpEC):

- Multi-domain pseudo-spectral method.

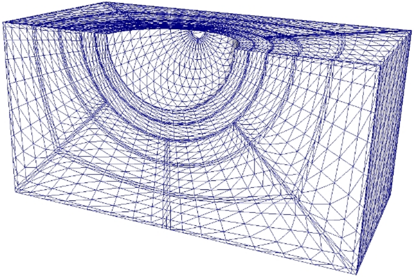

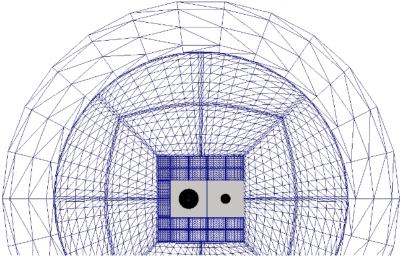

- Constraint damped "generalized harmonic" Einstein equations:

$$\Box g_{ab} = F_{ab}(g, \partial g).$$

- Constraint-preserving, physical and gauge boundary conditions.

Moving Black Holes

- Black hole interior is not in causal contact with exterior. Interior is removed, introducing an excision boundary.

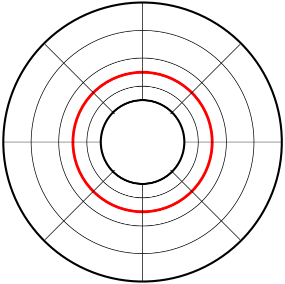

Moving Black Holes

- Black hole interior is not in causal contact with exterior. Interior is removed, introducing an excision boundary.
- Numerical grid must be moved when black holes move too far.

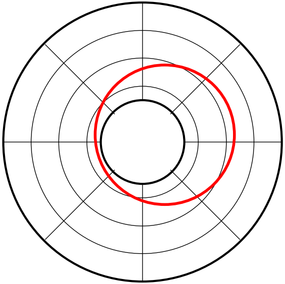

Moving Black Holes

- Black hole interior is not in causal contact with exterior. Interior is removed, introducing an excision boundary.
- Numerical grid must be moved when black holes move too far.

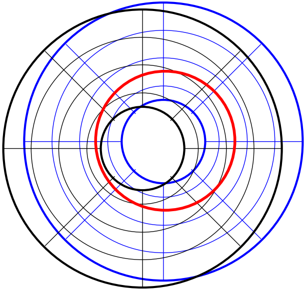

Moving Black Holes

- Black hole interior is not in causal contact with exterior. Interior is removed, introducing an excision boundary.
- Numerical grid must be moved when black holes move too far.

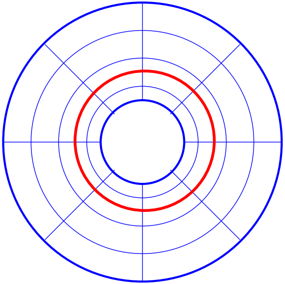

Moving Black Holes

- Black hole interior is not in causal contact with exterior. Interior is removed, introducing an excision boundary.
- Numerical grid must be moved when black holes move too far.
- Problems:
  - Difficult to get smooth extrapolation at trailing edge of horizon.

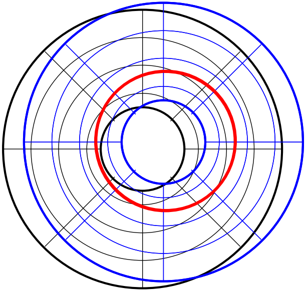

Moving Black Holes

- Black hole interior is not in causal contact with exterior. Interior is removed, introducing an excision boundary.
- Numerical grid must be moved when black holes move too far.
- Problems:
  - Difficult to get smooth extrapolation at trailing edge of horizon.
  - Causality trouble at leading edge of horizon.

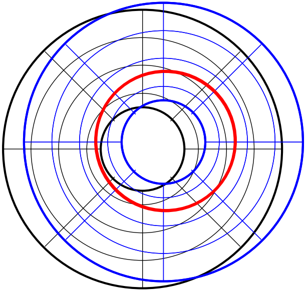

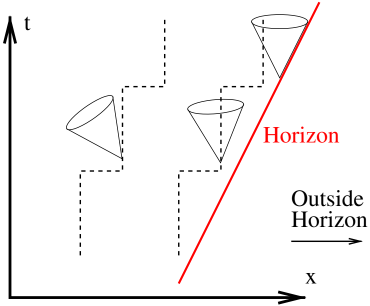

Moving Black Holes

- Black hole interior is not in causal contact with exterior. Interior is removed, introducing an excision boundary.
- Numerical grid must be moved when black holes move too far.
- Problems:
  - Difficult to get smooth extrapolation at trailing edge of horizon.
  - Causality trouble at leading edge of horizon.
- Solution:
  Choose coordinates that smoothly track the motions of the centers of the black holes.

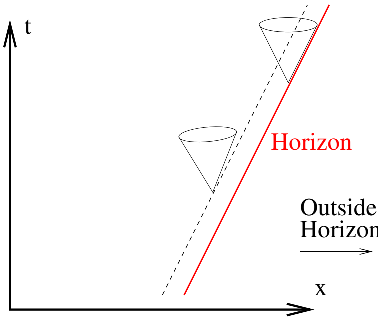

Horizon Tracking Coordinates

- Coordinates must be used that track the motions of the holes.
- A coordinate transformation from "inertial" coordinates, $(\bar{x}, \bar{y}, \bar{z})$, to "co-moving" coordinates (x, y, z), consisting of a rotation followed by an expansion,

$$\begin{pmatrix} x \\ y \\ z \end{pmatrix} = e^{a(\bar{t})} \begin{pmatrix} \cos\varphi(\bar{t}) & -\sin\varphi(\bar{t}) & 0 \\ \sin\varphi(\bar{t}) & \cos\varphi(\bar{t}) & 0 \\ 0 & 0 & 1 \end{pmatrix} \begin{pmatrix} \bar{x} \\ \bar{y} \\ \bar{z} \end{pmatrix},$$

  is general enough to keep the holes fixed in co-moving coordinates for suitably chosen functions $a(\bar{t})$ and $\varphi(\bar{t})$.
- Since the motions of the holes are not known *a priori*, the functions $a(\bar{t})$ and $\varphi(\bar{t})$ must be chosen dynamically and adaptively as the system evolves.

Horizon Tracking Coordinates II

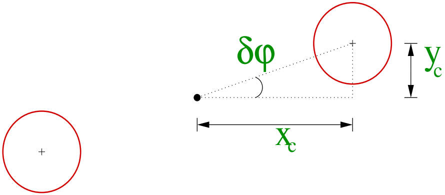

- Measure the co-moving centers of the holes: $x_c(t)$ and $y_c(t)$, or equivalently

$$
\begin{aligned}
Q^x(t) &= \frac{x_c(t) - x_c(0)}{x_c(0)},\\
Q^y(t) &= \frac{y_c(t)}{x_c(t)}.
\end{aligned}
$$

Horizon Tracking Coordinates II

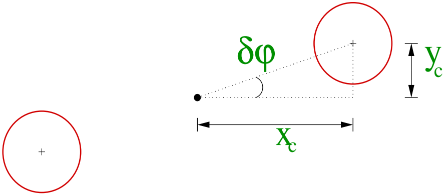

- Measure the co-moving centers of the holes: $x_c(t)$ and $y_c(t)$, or equivalently

$$
\begin{aligned}
Q^x(t) &= \frac{x_c(t) - x_c(0)}{x_c(0)}, \\
Q^y(t) &= \frac{y_c(t)}{x_c(t)}.
\end{aligned}
$$

- Use a feedback-control system to adjust the map parameters $a(t)$ and $\varphi(t)$ in such a way that $Q^x(t)$ and $Q^y(t)$ remain small, thus keeping the positions of the black holes at fixed coordinate locations along the x axis.

Horizon Distortion Maps

- Tidal deformation, along with kinematic and gauge effects cause the shapes of the black holes to deform:

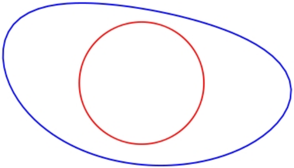

Horizon Distortion Maps

- Tidal deformation, along with kinematic and gauge effects cause the shapes of the black holes to deform:

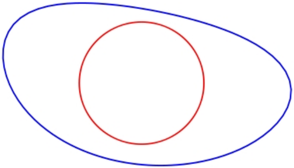

- If the holes become significantly distorted – relative to the spherical excision surface – bad things happen:
  - Some points on the excision boundary are much deeper inside the singular black hole interior. Numerical errors and constraint violations are largest there, sometimes leading to instabilities.

Horizon Distortion Maps

- Tidal deformation, along with kinematic and gauge effects cause the shapes of the black holes to deform:

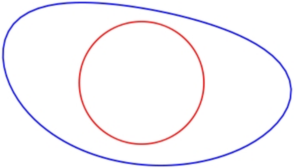

- If the holes become significantly distorted – relative to the spherical excision surface – bad things happen:
  - Some points on the excision boundary are much deeper inside the singular black hole interior. Numerical errors and constraint violations are largest there, sometimes leading to instabilities.
  - When the horizons move relative to the excision boundary points, the excision boundary can become timelike, and boundary conditions are then needed there.

Horizon Distortion Maps II

- Adjust the placement of grid points near each black hole using a horizon distortion map that moves grid coordinates x^i into points in the black hole rest frame $\tilde{x}^i$:

$$
\begin{aligned}
\tilde{\theta}_A &= \theta_A, \qquad \tilde{\varphi}_A = \varphi_A, \\
\tilde{r}_A &= r_A - f_A(r_A, \theta_A, \varphi_A) \sum_{\ell=0}^{L} \sum_{m=-\ell}^{\ell} \lambda_A^{\ell m}(t) Y_{\ell m}(\theta_a, \varphi_A).
\end{aligned}
$$

- Adjust the coefficients $\lambda_A^{\ell m}(t)$ using a feedback control system to keep the excision surface the same shape and slightly smaller than the horizon.
- Choose f_A to scale linearly from $f_A = 1$ on the excision boundary, to $f_A = 0$ on the surrounding cube.

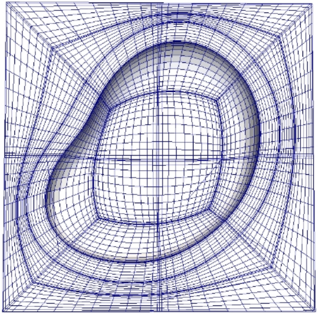

Dynamical Gauge Conditions

- The spacetime coordinates x^b are fixed in the generalized harmonic Einstein equations by specifying H^b:

$$\nabla^a \nabla_a x^b \equiv H^b.$$

- The generalized harmonic Einstein equations remain hyperbolic as long as the gauge source functions H^b are taken to be functions of the coordinates x^b and the spacetime metric g_{ab}.
- The simplest choice $H^b = 0$ (harmonic gauge) fails for very dynamical spacetimes, like binary black hole mergers.
- We think this failure occurs because the coordinates themselves become very dynamical solutions of the wave equation $\nabla^a \nabla_a x^b = 0$ in these situations.
- Another simple choice – keeping H^b fixed in the co-moving frame of the black holes – works well during the long inspiral phase, but fails when the black holes begin to merge.

Dynamical Gauge Conditions II

- Some of the extraneous gauge dynamics could be removed by adding a damping term to the harmonic gauge condition:

$$\nabla^a\nabla_a x^b = H^b = \mu t^a \partial_a x^b = \mu t^b = \mu g^{bt}/\sqrt{-g^{tt}}.$$

- This works well for the spatial coordinates x^i, driving them toward solutions of the spatial Laplace equation on the timescale $1/\mu$.

Dynamical Gauge Conditions II

- Some of the extraneous gauge dynamics could be removed by adding a damping term to the harmonic gauge condition:

$$\nabla^a\nabla_a x^b = H^b = \mu t^a\partial_a x^b = \mu t^b = \mu g^{bt}/\sqrt{-g^{tt}}.$$

- This works well for the spatial coordinates x^i, driving them toward solutions of the spatial Laplace equation on the timescale $1/\mu$.
- For the time coordinate t, this damped wave condition drives t to a time independent constant, which is not a good coordinate.
- A better choice sets H_t proportional to $\mu \log \sqrt{-\det g_{ij}/g^{tt}}$. This time coordinate condition keeps the ratio $\det g_{ij}/g^{tt}$ close to unity, even during binary black hole mergers where it becomes of order 100 using our simpler gauge conditions.

Generic Mergers

- Recent improvements now allow the Caltech/Cornell code SpEC to perform inspiral merger and ringdown simulations robustly for a wide range of black hole binary systems.

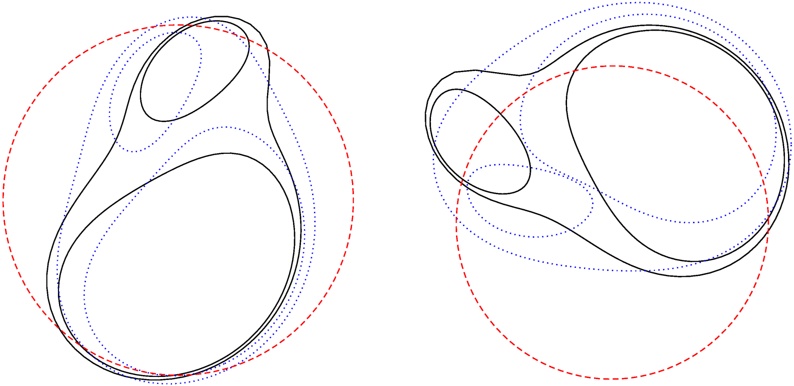

Numerical BBH Gravitational Waveforms

- The Caltech/Cornell collaboration has computed high precision numerical inspiral-merger-ringdown waveforms for several simple equal-mass BBH systems.

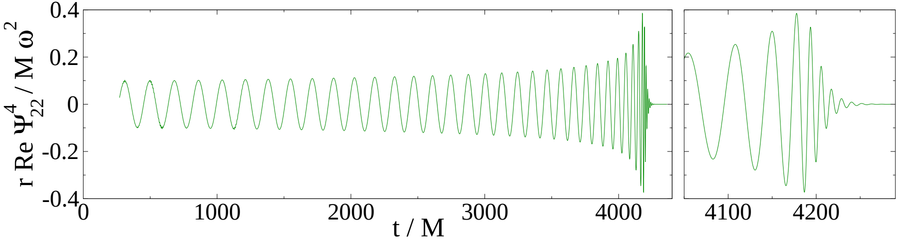

- Do these waveforms meet the required accuracy standards for LIGO data analysis?

Determining Numerical Waveform Accuracy

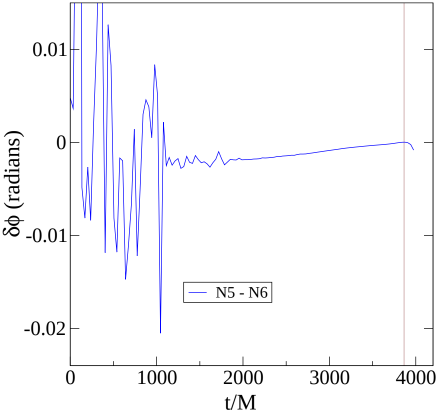

- Numerical convergence of gravitational waveform.

Determining Numerical Waveform Accuracy

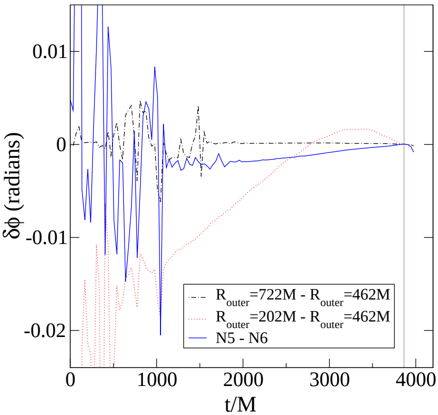

- Numerical convergence of gravitational waveform.
- Phase dependence on outer boundary location.

Determining Numerical Waveform Accuracy

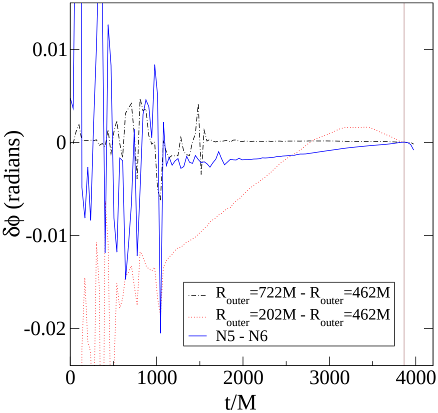

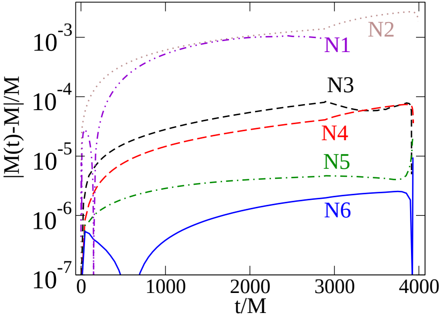

- Numerical convergence of gravitational waveform.
- Phase dependence on outer boundary location.

- Constancy of the black hole masses.

Summary of Numerical Waveform Phase Errors:

Effect	$\delta\phi$ (radians)
Numerical truncation error	0.003
Finite outer boundary	0.005
Drift of mass M	0.002
Extrapolation $r \to \infty$	0.005
Wave extraction at $r_{\rm areal}$=const?	0.002
Coordinate time = proper time?	0.002
Lapse spherically symmetric?	0.01
root-mean-square sum	**0.01**

Summary of Numerical Waveform Phase Errors (Including Physical Parameter Errors):

Effect	$\delta\phi$ (radians)
Numerical truncation error	0.003
Finite outer boundary	0.005
Drift of mass M	0.002
Extrapolation $r \to \infty$	0.005
Wave extraction at $r_{\rm areal}$=const?	0.002
Coordinate time = proper time?	0.002
Lapse spherically symmetric?	0.01
residual orbital eccentricity	0.02
residual black hole spin	0.03
root-mean-square sum	**0.04**

Summary of Numerical Waveform Phase Errors (Including Physical Parameter Errors):

Effect	$\delta\phi$ (radians)
Numerical truncation error	0.003
Finite outer boundary	0.005
Drift of mass M	0.002
Extrapolation $r \to \infty$	0.005
Wave extraction at r_{areal}=const?	0.002
Coordinate time = proper time?	0.002
Lapse spherically symmetric?	0.01
residual orbital eccentricity	0.02
residual black hole spin	0.03
root-mean-square sum	**0.04**

It isn't known yet whether these waveforms meet the real frequency domain waveform accuracy standards required for LIGO data analysis.